AIAA JOURNAL
Vol. 49, No. 4, April 2011

Subsonic Jet Mixing via Active Control Using Steady and Pulsed Control Jets

Muhammad A. Kamran* and James J. McGuirk†
Loughborough University, Loughborough, England LE11 3TU, United Kingdom

DOI: 10.2514/1.J050608

A comparison of the performance of steady and pulsed control jets in enhancing the mixing rate of a high Reynolds number (10^6) high subsonic Mach number (0.9) jet is reported. The key parameters affecting control jet performance are identified as control jet pressure ratio, Strouhal number (St), and mode number (m), and an existing nozzle test facility is modified to allow detailed investigation of these parameters. Optimization of the control jet design lead to increased mixing, such that a primary jet potential core length reduction of 50% was achieved. The increase in jet/ambient entrainment interfacial area was seen as an important factor. Pulsation at $St = 0.22$ in an antisymmetric mode ($m = 1$) gave the best results. The data provided, based on extensive laser Doppler anemometry mean velocity and turbulence measurements, allowed an improved understanding of the physical processes that are crucial for enhanced mixing and contribute a useful new data set for computational fluid dynamics validation of rapid mixing jet flows.

Nomenclature

d	=	control jet nozzle exit diameter, m
D_n	=	primary jet nozzle exit diameter, m
D_S	=	diameter of rotating shaft, m
d_h	=	diameter of hole drilled in rotating shaft, m
f	=	control jet pulsation frequency, Hz
m	=	azimuthal mode number
St	=	Strouhal number, fD_n/U_j
St_{opt}	=	optimum Strouhal number
T	=	time period of pulse, s
U	=	local mean axial velocity, m/s
U_{cj}	=	control jet nozzle exit centerline mean axial velocity, m/s
U_j	=	primary jet nozzle exit centerline mean axial velocity, m/s
x	=	axial direction, m
y	=	horizontal (spanwise) direction, m
z	=	vertical (transverse) direction, m
α	=	duty cycle, %
ρ_{cj}	=	control jet nozzle exit centerline density, kg/m^3
ρ_j	=	primary jet nozzle exit centerline density, kg/m^3
τ	=	pulse width, s

I. Introduction

THERE is much current interest in methods for manipulation (usually enhancement) of the mixing between aeroengine jet exhaust plumes and the surrounding ambient air. Two major benefits of enhanced mixing are noise reduction in civil transport operations and infrared (IR) signature reduction for low observable military aircraft. The latter is the primary application driver of the current study, and a recent overview of work in this area has been provided by Knowles and Saddington [1]. In particular, we investigate here the effectiveness of control jets (hereafter referred to as CJs), both steady and pulsed, used to achieve mixing enhancement of a primary (thrust-producing) jet at high Reynolds and Mach numbers typical of engineering practice. The largest source of IR radiation in combat aircraft is the engine afterburner and exhaust nozzle, where surface and gas temperatures are greatest. Enhanced mixing with the ambient of the propulsion system exhaust plume decreases the plume temperature and suppresses IR radiation. Decreased plume temperature will also reduce the temperature of the aerodynamic surfaces with which the plume interacts, providing greater flexibility in the choice of manufacturing materials for these components. Considerable effort has thus been invested into research on mixing enhancement techniques. There is clearly a tradeoff exercise to be carried out, since many devices that increase mixing will also incur a thrust loss penalty; only approaches that offer an appropriate balance between these two aspects are likely to be considered in real engine applications. The following is a brief review of some that have shown promise.

Jet mixing techniques may be divided into two major categories: passive and active. Passive techniques input no energy into the flow and are usually associated with exhaust nozzle geometric modifications. These range from alterations in the exit shape of the jet nozzle [2,3] to the implementation of toothlike tabs [4,5] or vortex generators (VGs) [6,7] introduced near the nozzle exit. Active techniques, on the other hand, inject energy into the flow, for example, via one or more CJs discharged at an angle to the primary propulsion jet close to the nozzle exit. The CJs can be operated either under steady flow conditions or pulsate at a specific predefined frequency (open-loop control) or at a frequency that is based on some feedback signal in the flow (closed-loop control). Acoustic controllers [8], oscillating, forced momentum (pulsed) jets [9], and piezoelectric generators [10] are among the active mixing techniques that have been explored. In achieving closed-loop active control, CJ operating conditions (e.g., velocity amplitude, frequency modulation, and phase) would be continuously updated through a feedback loop, an approach which offers, in principle, increased flexibility and potential for influencing primary jet flow behavior. However, such systems in the exhaust plume application are inherently difficult to design. Any feedback signal would have to be obtained from a sensor that detected the flow behavior in the first 10 diameters or so of plume development downstream of the nozzle exit. For this reason, closed-loop systems have not yet clearly demonstrated their potential convincingly, and they are not being actively studied at present.

The use of solid tabs/VGs has long been considered the most effective passive technique for increasing the jet mixing rate. Since

Received 16 April 2010; revision received 10 September 2010; accepted for publication 8 November 2010.

*Research Student, Department of Aeronautical and Automotive Engineering; currently Assistant Professor, Mechanical Engineering Department, NWFP University of Engineering and Technology, Peshawar 2500, Pakistan.

†Professor of Aerodynamics, Department of Aeronautical and Automotive Engineering.

the initial work by Bradbury and Khadem [4], the works of Zaman et al. [11], Behrouzi and McGuirk [12], Foss and Zaman [13], Bohl and Foss [14], and Hu et al. [15], among others, have established that the creation of strong streamwise vortex motions is responsible for the enhanced mixing, although the precise mechanisms are still not completely established. Tabs/VGs introduce a drag or thrust loss penalty, which needs to be minimized as far as possible. This has lead to alternative approaches for introduction of streamwise vortices. Injection of streamwise vorticity, without using solid tabs/VGs, has been used as a flow control mechanism for other aerodynamic applications, such as boundary-layer separation control. Johnston and Nishi [16] studied air jet VGs (AJVGs), which are several CJs injected transversely to the main flow to create embedded regions of streamwise vorticity, as an alternative to solid VGs for boundary-layer flow control. Bray and Garry [17] present experimental data that show that AJVGs/CJs can be at least as effective as conventional vane-type VGs on aerofoils at high angles of attack to control separation.

The fact that CJs can be turned off when not required has encouraged researchers to explore this option for jet plume mixing and noise control. Davis [18] was the first to explore this technique for jet mixing by placing a pair of steady CJs 180° apart at the exit of a nozzle to simulate the same effect as solid tabs. Local velocity reductions of up to 30% for jet Mach numbers up to 0.7 were achieved with CJ mass flow rates of as little as 0.5% of the primary jet, as long as the CJs penetrated the shear layer of the primary jet. In these first CJ tests for primary jet mixing control, the CJ size and momentum was, however, chosen to be so large that a significant blockage/primary jet mass flow reduction was recorded. Such evidence of significant thrust loss would certainly be unacceptable for practical application. Lardeau et al. [19] studied the mixing process in the near-field region of a supersonic/subsonic mixing layer excited by a single steady transverse CJ with a velocity ratio of $U_{\mathrm{cj}}/U_j = 0.89$. Visualization of the flow using a particle image velocimetry (PIV) system showed intermittent depth of penetration of the CJ into the supersonic/subsonic mixing layer. Similar observations were made by Collin et al. [20], who studied the effect of a steady CJ on a supersonic mixing layer through a combination of visualization and laser Doppler anemometry (LDA) measurements. They observed that the CJ oscillated between deep penetration and complete blockage by the primary flow, resulting in a periodic penetration process that had a strong influence on the manipulated mixing-layer structures. Behrouzi and McGuirk [21] referred to their steady CJs as fluid tabs to emphasize their similar streamwise vorticity enhanced mixing mechanism to that found with solid tabs, and they compared their performance with solid tabs in enhancing mixing of an axisymmetric jet flow. They found that the effectiveness of the CJs depended strongly on penetration, which was primarily a function of CJ/primary jet velocity ratio. CJ penetration slightly greater than the nozzle exit boundary-layer thickness enabled strong interaction with the primary jet shear layer and produced similar effects on the jet mixing and spreading rate as solid tabs. Recently, Chauvet et al. [22] numerically investigated 1) the effect of the number of steady CJs distributed around the nozzle periphery (two to eight were explored) and 2) the total pressure of the injected CJ air on the mixing enhancement of a moderately underexpanded primary jet at a nozzle pressure ratio (NPR) of 3.1. They noted that four CJs were, marginally, most efficient in spreading the jet, but this lead to a higher thrust loss compared with two CJs, which in fact achieved almost the same enhanced spreading performance as the four-CJ configuration. The preference for a small number of mixing-layer excitation sites had already been observed in solid tab studies by Behrouzi and McGuirk [21] and explained as beneficial by delaying the mutual interaction between the streamwise vortex systems introduced by neighboring CJs for as long as possible.

All the preceding work used steady CJs; pulsed CJs contain periodic oscillations superimposed on a mean continuous flow rate. It has been observed several times that, for maximum effectiveness, the excitation frequency of the pulsation should fall within a target range. The preferred frequency f is characterized via an optimum Strouhal number ($St_{\mathrm{opt}} = fD_n/U_j$). Many researchers have experimentally observed that there is a surprisingly wide range for St_{opt} (0.2–0.6), but it is often concluded to be optimally effective close to 0.3. This corresponds to an overall primary jet columnar instability frequency (Crow and Champagne [23]) rather than any mechanism associated with nozzle lip boundary-layer/shear-layer instability. Researchers have therefore explored the performance of pulsed CJs for increased mixing in jets and shear layers. Raman and Cornelius [9] provided the first investigation of this technique, using two transversely oscillating fluidic jets to excite a low Re (10^5) rectangular primary jet. Because of experimental limitations, only excitation at the first subharmonic of the preferred columnar instability mode was effected, with the CJs operating in-phase to generate a sinuous mode of forcing and out-of-phase to create a varicose mode. A 35% reduction in potential core length and a 60% increase in the primary jet mass flux at downstream stations in the jet near field were achieved compared with an unexcited (clean) jet. It is likely, however, that these experiments were more effective at forcing large-scale global primary jet flapping as opposed to using the CJs to create streamwise vorticity enhanced mixing. Parekh et al. [24] were the first to apply the pulsed CJ technique to enhance mixing in round jets relevant to the aeroengine application. The velocity from two radially oriented slot jets was pulsed in symmetric mode (in-phase) and antisymmetric mode (180° out-of-phase from each other) with peak velocities ~30% of the primary jet velocity (~2% of primary mass flow) to excite large-scale oscillations in the primary jet. Once again (perhaps following the work of [9]), only the first subharmonic $St = 0.15$ was studied. A large increase in the spreading rate of the primary jet was achieved; the data showed that pulsed CJs were extremely effective in reducing the potential core length (a factor of two) and that pulsed CJs were more effective in antisymmetric rather than symmetric excitation mode. These tests were sufficiently promising, and the technique was also trialed on a full-scale engine with similar results [25]. The work of Ibrahim et al. [26], using a primary jet at $Re = 1.5 \times 10^5$, also showed that antisymmetric injection caused a higher spreading rate than either steady or unsteady symmetric injection in terms of centerline velocity decay. However, ignoring the knowledge gained from tab flow studies on optimum vorticity source numbers, the experiments of [26] used 12 CJs ($d/D_n = 1/15$) placed around the circumference of a convergent nozzle to excite the jet flow. Different configurations of steady and unsteady, and symmetric and antisymmetric modes were studied for a fully expanded ($M = 1$) primary jet. Only minor effects of steady CJs on the primary jet were observed, probably because of the low individual CJ momentum ratio tested (i.e., too large a number of CJs for the given CJ NPR). For pulsed CJs, these were again only operated at the first subharmonic, following [9,24]. In addition, the NPR of the CJs was increased to match the time-averaged mass flow rate of pulsed CJs and steady CJs. This practice raises some difficulties in comparing pulsed and steady CJ performance since, to achieve equal mass flow rates, the peak velocity amplitude for pulsed CJs is almost twice that of steady CJs. Hence, any increased benefits attained with pulsed CJs cannot be solely attributed to the pulsing action but are a combined effect of both higher amplitude and unsteady pulsation. A better way to judge if pulsed CJs are superior to steady CJs is to keep the peak amplitude of pulsed CJ velocity equal to the steady CJ velocity (this practice is adopted in the current study, see Sec. II). Results of the mean flowfield from [26] showed pulsed antisymmetric injection (the bottom six actuators operated 180° out of phase with respect to the top six) caused a higher spreading rate than either steady or unsteady symmetric injection in terms of potential core reduction (41% shorter for the antisymmetric case) and jet radius increase. No turbulence data were gathered, and it was claimed that no bifurcation of the primary jet was observed, but radial profile measurements were only presented along one plane and at only three axial stations, which makes it difficult to substantiate this claim. The total CJ mass flow rate of 4% of the primary jet used for the majority of tests also makes this study of little direct relevance to practical applications, since this amount of engine bleed would result in an unaffordable thrust loss penalty. The CJ mass flow rate could be reduced and their effectiveness increased by lowering the number of CJs used. These considerations motivated the studies of Behrouzi

and McGuirk [27] and Behrouzi et al. [28], who chose to implement only two CJs and to limit the CJ mass flow requirement to 0.5–1% of the primary flow, adjusting the CJ nozzle diameter to obtain a velocity ratio of $U_{cj}/U_j \sim 1$ in order to ensure adequate CJ penetration and maximum interaction between CJ flow and primary jet shear layer. The data obtained showed that mixing effectiveness with a pair of pulsed CJs 180° out of phase was as good as achieved with a pair of solid tabs for a total CJ mass flow rate of only 0.5% of the primary jet. The performance of the pulsed CJs was strongly influenced by the CJ flow rate, pulse frequency, and phase, and these parameters had to be carefully chosen for optimal performance (i.e., maximum increased mixing for minimum CJ mass flow rate and minimum primary jet thrust loss).

For pulsed CJs, there are additional system parameters that can be tuned in addition to the Strouhal number to improve system performance. Johari et al. [29] studied the effect of duty cycle α (the percentage of time the CJ is on during each pulsation cycle) and pulse width (injection time) τ on the penetration and mixing of a pulsed transverse jet in crossflow; that is, rather than use pulsed CJs added to a primary jet, a single CJ was pulsed and injected at 90° into a steady cross-flowing stream. These parameters are, of course, related to each other:

$$\alpha = \tau/T \quad \text{or} \quad \tau = \alpha/f \tag{1}$$

where T is the time period and f is the frequency of the pulsation cycle. Johari [30] argued that the amount of CJ fluid ejected during each pulse and the separation between successive ejections are the two fundamental parameters governing the dynamics of strongly pulsed jets in crossflow. For a fixed CJ velocity and diameter, duty cycle and pulse width are therefore the parameters that control the jet structure and trajectory; however, to date for enhanced primary jet mixing flows, there has been little study of the influence of duty cycle/pulse width on CJ performance.

Although the work detailed previously on pulsed CJs has identified the parameters that affect their performance, most of these studies were either carried out in water (to ease the task of achieving the relevant St values) [27–30] or in air, with the primary jet operating in the incompressible regime [9,24]. Only [26–28] used primary jets with high Re and Mach numbers. For the high Re/Mach range relevant to aeroengine practice, the required CJ authority (i.e., CJ mass flow) and optimum excitation frequency both increased substantially in absolute magnitude terms. This is the main reason why early attempts at using acoustic excitation have not proven feasible for such applications, since the required frequency level introduces limitations in weight, power, and maintenance of the acoustic drivers. Technology for pulsing CJs driven by engine bleed air with the high bandwidth and high amplitude demanded by engine-relevant operating conditions is also a potential problem. For this reason, electromagnetic flap actuators have been explored in the recent work of Suzuki et al. [31]. Samimy et al. [32–34] and Kim et al. [35] have reported the development of localized arc filament plasma actuators (LAFPAs) to excite high-Mach-number primary jets. The latter development is based on the idea that repetitive pulsing of plasma actuators causes rapid heating of the air near the nozzle wall at exit, creating a small region of high-momentum fluid, which can be used to interact with the primary jet flow and to excite the primary jet shear layer. In this sense, this technique is based on a similar flow interaction mechanism to CJs, but it has the technological benefits of being able to generate high frequencies with ease and does not require any engine bleed air. Although the work reported in [32–35] was primarily motivated by noise mitigation (civil aeroengine applications) rather than the enhanced mixing/IR reduction application of interest here, the experiments performed have many overlapping features with forced CJ flows.

Kim et al. [35] used an array of eight LAFPAs, equally distributed azimuthally just upstream of a primary nozzle exit plane, to study the effect of frequency and azimuthal mode variations on a Mach 0.9 jet with a Reynolds number of 7.6×10^5 using PIV. According to Parekh et al. [24], the azimuthal mode m is one where actuation is controlled such that in one actuation cycle, the perturbation introduced travels an azimuthal distance of $2\pi m$. For multiple actuators distributed with $\Delta\theta°$ between two consecutive actuators, the phase angle for mode m is defined as $\phi_m = m\theta$ relative to the actuator at $\theta = 0°$. With eight actuators, azimuthal modes $m = 0$, 1, 2, 3, and 4 can be excited. Mode $m = 0$ is the symmetric mode of excitation (all actuators in phase). Positive or negative mode numbers are used to describe the direction of rotation (e.g., positive—clockwise/negative—anticlockwise). For just two actuators, $m = +1$ and $m = -1$ modes are indistinguishable, and this is referred to as the $m = 1$ or antisymmetric mode here. Mixed modes (e.g., $m = \pm 1$) are possible by the addition of two modes rotating in opposite directions. A wide Strouhal number range of 0.09–3.08 was studied to cover both jet columnar and shear-layer instabilities. Maximum spreading of the primary jet occurred in a Strouhal number range of 0.2–0.4, when the large scale structures generated by the excitation were very well organized and their length scales were comparable to the primary nozzle diameter by the end of the potential core. An investigation of the azimuthal modes of excitation in the St range of 0.2–0.4 showed an increase in spreading for all modes compared with the clean jet, but a mixed antisymmetric mode ($m = \pm 1$) was claimed to be the most effective. This mode was synthesized by grouping together the top three actuators and the bottom three actuators and operating these two groups 180° out of phase while leaving the two remaining actuators inoperative. Note that this does not correspond precisely to the $m = \pm 1$ mode as defined by [24], since the amplitude difference (factor of two) between the actuators required for a mixed $m = +1$ and $m = -1$ mode was not realized in the experiments: this was not technically feasible with LAFPAs. A further constraint of the plasma actuating technology was the limited independent control of duty cycle value (α). Although it is stated that a range of values was studied, only results for the rather low value of 5–10% are presented, since this apparently provided the best results. The precise interpretation of the duty cycle value is also open to question, since α could only be determined from the plasma actuator electrical signal characteristics, rather than local overpressure or velocity perturbation data, which are more usual for determining duty cycle from an aerodynamic perspective. As mentioned previously, more data on the influence of α in enhanced jet mixing flows are certainly needed. Finally, the superiority of the $m = \pm 1$ mode over all other modes in enhancing the spread of the shear layers, as concluded in [35], might be misleading. In the implementation of the mixed antisymmetric mode, as described in [35], the two actuator groups could realistically be considered as two single actuators operating with a phase difference of 180° (i.e., a pure $m = 1$ mode) but spanning a much larger azimuthal area and producing a significantly higher forcing momentum flow due to their combined effect at any instant of time.

The work described in the present paper aims to add to the body of work on CJ-enhanced mixing described previously. While many investigations on unsteady excitation of primary jet shear layers have been reported, and a substantial and fundamental understanding of the important mechanisms has been established, much of the reported work, for experimental convenience, has focused on low primary jet $Re(\sim 10^4)$ and, often, low Mach number (<0.3) or even incompressible flow. While the Mach number is not thought to exert a strong influence on CJ-induced enhanced mixing mechanisms, it is important that the effectiveness of any enhancement technique be demonstrated at Re and M values representative of the engineering application if the technique is to be considered seriously by designers. For the relevant range of high Re/M, the effectiveness of pulsed CJs at the high frequencies needed has had only sparse attention (most reported studies have used LAFPAs). An experimental study is therefore reported here into the use of steady and open-loop control pulsed CJs for manipulation of high subsonic ($M = 0.9$), high $Re(Re = 10^6)$ primary jet plume development. The main objective of the present study was to provide sufficiently detailed mean velocity and turbulence data in the primary jet near field ($x/D_n < 10$) to allow the performance of steady and pulsed injection on mixing enhancement to be captured, as well as providing a data set suitable for computational fluid dynamics (CFD) validation studies of rapid mixing jet flow problems.

II. Experimental Techniques and Procedures

Experiments were carried out in the high-pressure nozzle test facility (HPNTF) at Loughborough University; this has been specially designed to permit study of single and coaxial (primary/secondary) subsonic and supersonic jet flows for a wide range of nozzle scales, geometries, and operating conditions up to NPRs of ∼5. Details of this facility are provided in Behrouzi and McGuirk [12,27] and Behrouzi et al. [28]. High-pressure air is provided at a steady flow rate of ∼1.0 kg/s from 15 bar (abs) screw compressors. The air is dried using a desiccant drier to a dew point of −40°C, then it is stored in two air reservoirs with a volume of ∼120 m^3. A 0.15-m-diam air supply pipeline delivers compressed air into the HPNTF test cell containing the nozzle rig (Fig. 1).

The air supply line contains a first-level control valve used to provide coarse regulation of the air pressure down to ∼5 bar. A second rig control valve is located inside the test cell (D in Fig. 1) and is automatically adjusted from a panel in the test cell control room to set and hold the NPR of the primary jet at a constant value to within an accuracy of ±1% during blowdown testing (when the nozzle size and NPR values require mass flow rates larger than 1.0 kg/s). The primary jet formed by the air discharging from the nozzle is available for detailed plume characterization for a distance of 1.5 m (typically 25 nozzle diameters) before entering a detuner for noise attenuation and exhaust. The nozzle used for the present tests (Fig. 1) was an axisymmetric convergent nozzle with an internal convergent half-angle of 11°, an exit diameter D_n of 60 mm, and a short (30 mm) parallel-walled section at nozzle exit to avoid vena contracta effects and provide a region for the nozzle wall boundary layer to recover from the relaminarizing effects of the internal nozzle acceleration. The Cartesian coordinate system used to report all the following data is also shown in Fig. 1.

The CJ air supply system for both steady and pulsed operation was arranged as follows: one of the HPNTF high-pressure air reservoirs was isolated once fully charged by means of a servo-controlled three-way valve. This then served as the high-pressure air supply for the CJs; a direct line connected the reservoir two small two-CJ feed blocks attached to the outer wall of the primary nozzle. A pressure regulator in the test cell control room was used to adjust the pressure of the CJ air supply and was monitored using an absolute pressure transducer. To account for any loss of total pressure in ductwork, the CJ NPR was monitored at a position close to the CJ nozzle exit on the inner wall of the primary nozzle. This was done using identical Kulite subminiature fast-response pressure transducers mounted in both CJ feed blocks, thus also allowing accurate time-resolved monitoring of each CJ NPR under pulsed operation. A mass flow meter with a range of 0–0.0086 kg/s was installed some distance upstream of the CJs to monitor the total steady-state flow rate of the CJs. For steady CJ flow operation, the pressure regulator was set to achieve a given NPR at the CJ nozzle exits. Flexible tubing was used to connect the air supply to the CJ nozzles; see Fig. 2 for two CJs placed at 12 and 6 o'clock positions ($z = \pm 0.5 D_n$).

The pulsation system was designed to excite the primary jet over a Strouhal number range of 0.1–0.5 for high subsonic jets, corresponding to a CJ pulsation range of 600–2000 Hz for the primary jet nozzle size and Mach number selected. These frequencies are much higher than frequencies that have been tested before for forced pulsed jets, and only plasma actuators [32–35] have been positively demonstrated as capable of exciting an $M = 0.9$ jet at these frequencies with sufficiently large peak amplitudes. In the current investigation, CJ pulsation at these frequencies was achieved using the shaft of a pneumatic power tool with a maximum rotation speed of 75,000 rpm. The rotating shaft contained an accurately drilled transverse hole, arranged to be positioned within the CJ feed block. When the shaft hole was suitably aligned with holes in the feed blocks, the high-pressure air was connected to the CJs, which were thus pulsed at a frequency/duty cycle set by the shaft/feed block hole geometry and shaft speed.

The shaft speed was controlled by two pressure regulators connected in series for coarse and fine control to adjust the shaft

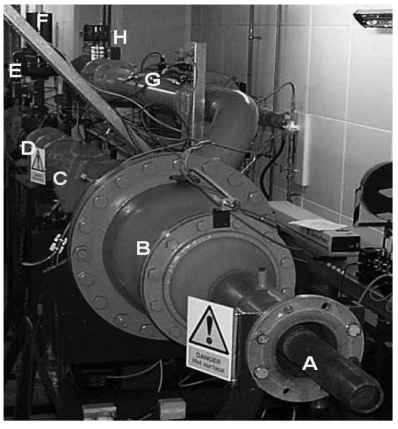

A	Primary nozzle delivery duct
B	Secondary flow plenum and contraction
C	Combustor
D	Primary control valve
E	Globe valve
F	Rig air supply pipe
G	Secondary flow supply pipe
H	Secondary control valve

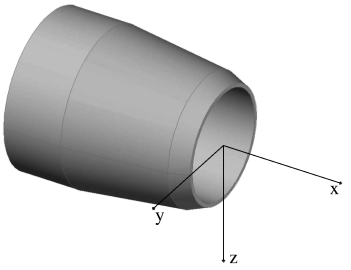

Fig. 1 HPNTF and primary jet nozzle geometry/reference coordinate system.

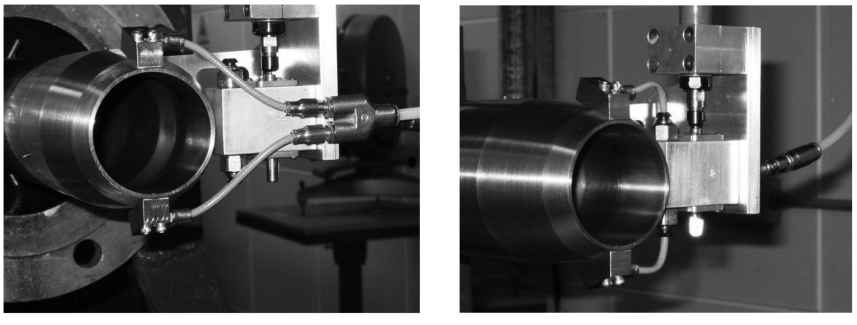

Fig. 2 CJ air supply system: steady jets (left) and pulsed jets (right).

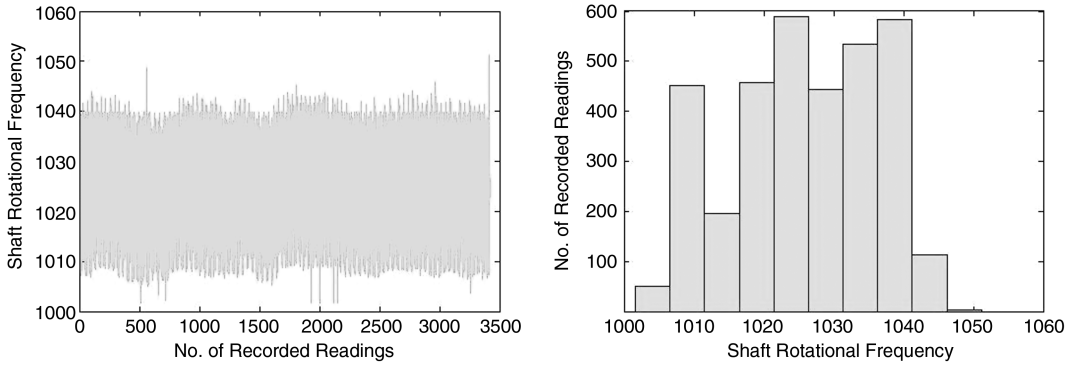

Fig. 3 Stability at shaft rotational frequency $f = 1025$ Hz.

revolutions per minute to the desired value. The frequency of CJ pulsation f was related to the shaft revolutions per minute N via

$$f = 2N/60 \tag{2}$$

Where the factor 2 shows one revolution of the shaft excited each CJ twice. Figure 2 (right) shows this system for two CJs connected to pulse in phase. To monitor the shaft revolutions per minute, a digital tachometer was employed. This provided instantaneous and average revolutions-per-minute values to an accuracy of $\pm 1\%$ in the range of 100–60,000 rpm. The stability of the rotating shaft revolutions per minute at different target CJ frequencies was checked by recording tachometer readings for periods of time ($\sim$6 min., the time to measure a complete centerline profile). This showed that the system remained very stable once set. The stability for a target frequency of 1025 Hz is shown in Fig. 3 (behavior similar at other frequencies).

While the preceding test checked the stability of the shaft rotation, a more direct option for monitoring CJ pulsation frequency and the waveform of the CJ exit velocity was to use the LDA system available in the HPNTF (see next for details) to record a time history of the instantaneous velocity at CJ exit (with the primary jet turned off) by tracking the velocity of each validated seeding particle recognized by the LDA system. This resulted in a direct measurement of CJ velocity amplitude and excitation frequency. For these LDA data to give an accurate temporal history picture of the CJ velocity waveform shape and frequency, a high data rate of seeding particles was required (if possible, an order of magnitude greater than the frequency of the pulsating system). In these tests, diethylhexyl-sebacate liquid was used to provide the LDA seed particles ($\sim$0.25 μm diameter) and data rates of approximately 15,000 s^{-1} were attained. A time history is shown in Fig. 4 for a frequency of 1030 Hz.

These data were converted to the frequency domain to identify the excitation frequency by performing a fast Fourier transform (FFT) analysis. Figure 5 shows the energy spectral density evaluated from the time series shown in Fig. 4 for $f = 1030$ Hz (similar results obtained at all test frequencies). The peak in the spectrum of CJ velocity data appears very close to the target frequency of 1030 Hz. However, the turbulent nature of the CJ flow means that broadband turbulent fluctuations also appear and make it difficult to identify clearly the frequency of the tonal component. It was thus decided that shaft revolutions-per-minute monitoring should be used to set the pulsed CJ operating condition.

Since the Strouhal number is a very important parameter in influencing the performance of pulsed CJs and, in any CFD predictions of the present data, specification of the CJ exit boundary condition would be an important requirement, one final investigation into the CJ total pressure signal produced by the designed pulsation system was carried out. The Kulite transducers installed in the CJ air supply, as described previously, were monitored and logged to record the time history of the CJ total pressure variation during pulsed operation. These tests were conducted at various shaft speeds to compare the frequency values obtained with the information using the techniques described previously. The values matched with frequencies obtained from the mechanical system, and it was thus further confirmed that the tachometer data were sufficiently accurate for setting pulsed CJ frequency. A pressure waveform and the associated frequency spectrum obtained from the transducer data are shown in Figs. 6 and 7.

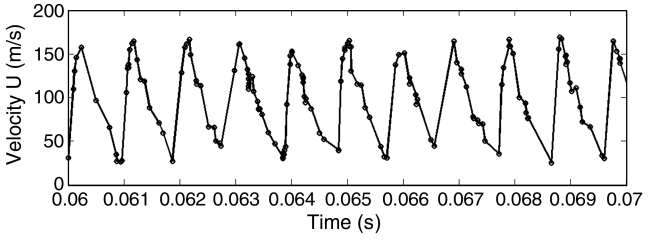

Fig. 4 LDA measured CJ velocity time history ($f = 1030$ Hz).

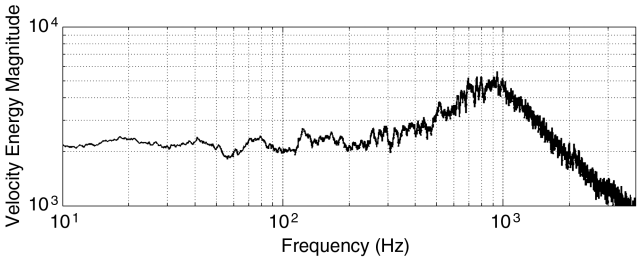

Fig. 5 FFT deduced frequency spectrum from LDA data ($f = 1030$ Hz).

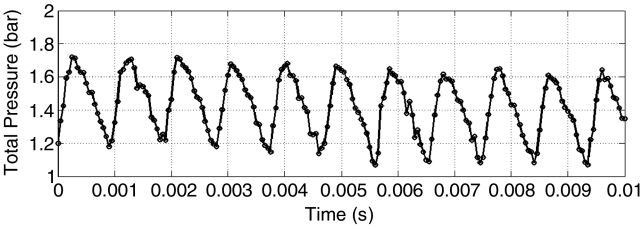

Fig. 6 CJ total pressure waveform from pressure transducer data ($f = 1030$ Hz).

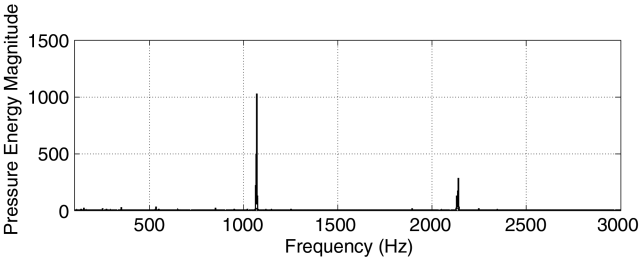

Fig. 7 FFT deduced frequency spectrum from pressure transducer data ($f = 1030$ Hz).

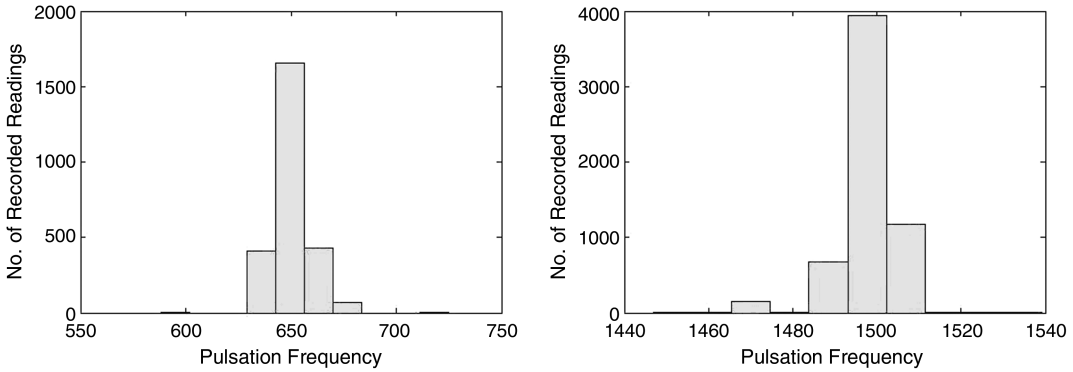

Fig. 8 Pulsation system operational checks: 650 (left) and 1500 Hz (right).

The frequency peak is clearly visible at a frequency of 1030 Hz, with the first harmonic also being detected. The system described previously was found to operate very satisfactorily over the desired frequency range, as shown in Fig. 8 for two frequencies of 650 and 1500 Hz.

It is the alternate blockage/opening of the air supply to the CJ nozzle caused by the shaft rotation that determines the pulsation frequency but also the duty cycle characteristics. In the present rotating shaft arrangement, the duty cycle α is related to rotating shaft diameter D_S and drilled hole diameter d_h via

$$\alpha = 4d_h/(\pi D_S) \tag{3}$$

Various duty cycles can thus be achieved by adjusting hole and shaft sizes. For the pulsed CJ tests reported here, only one duty cycle value was considered; viz., $\alpha = 0.64$ ($d_h = 4$ mm and $D_S = 8$ mm). The pulsation system also allowed control of the phase difference between the two CJs. This was achieved by drilling two transverse holes in the rotating shaft. These were oriented to be offset axially and perpendicular to each other circumferentially. The CJ feed block was modified to connect each CJ with a separate shaft hole, allowing operation 180° out of phase.

The primary jet was operated at an NPR of 1.70 (ambient temperature 288 K), producing a Mach 0.9 jet plume. The Reynolds number based on the nozzle diameter and the LDA measured centerline velocity at the nozzle exit plane was 1.15×10^6. The parallel extension to the nozzle ensured that the nozzle exit boundary layer was fully turbulent. Two CJs of 2 mm diameter placed 180° apart in the z-axis direction (Fig. 2) were introduced at the nozzle exit plane. This CJ size had previously been found effective in preliminary experiments by Behrouzi and McGuirk [27] and Behrouzi et al. [28] when operated with a small CJ mass flow ratio (0.13% of the primary jet mass flow rate through each CJ for a CJ supply pressure of 2 bar). Steady CJ tests were hence conducted at two different pressures, 2 and 3 bar (abs), while the pulsed CJ tests were conducted at a supply pressure of 2 bar. The steady CJ operating pressure was set by calculating the mean of 16,000 pressure readings from the Kulite transducers over a period of 1 s. For pulsed CJ tests, the operating pressure was set using the same method but by first setting the rotating shaft in the fully on position. This was done to enable comparison of the performance of steady and pulsed CJs for the same peak pressure. The pulsed jets were operated with $\alpha = 0.64$ at frequencies of 480, 1055, and 1920 Hz, corresponding to Strouhal numbers of 0.10, 0.22, and 0.40. The jet columnar and shear-layer frequencies for the present experiment were ~1400 and 120,000 kHz, respectively, showing that the present tests were clearly focused on excitation surrounding the jet columnar frequency, as in previous published works [33,35]).

The velocity field in the primary jet plume was measured using the LDA technique. The LDA system was a Dantec two-component (blue/green laser beam pairs) fiber-optic system made up of a 4 W argon ion laser source, a beam transmitter, and a signal processor (BSA F80) specially designed for high-speed flow measurement. Alumina powder, with an average size of 0.3 μm, was used during the plume velocity measurements to give a better signal/noise ratio. Velocity and turbulence profiles were captured by traversing the LDA measuring volume along the centerline of the plume, as well as across its diameter at several locations downstream of nozzle exit. Typical validated data rates were $\mathcal{O}$(1–10 kHz), depending on location; at each measurement point, data were gathered for a duration of 5 s or when 15,000 samples had been taken, whichever came first. Typical run times were 4–5 min. for radial traverse and 5–6 min. for axial traverse measurements. The overall uncertainty of the measurements due to statistical, velocity bias, and particle lag errors was estimated (see [36] for details) to be ±2%. With the equipment available, no phase-locked measurements were possible, so only time-averaged statistics are presented next; no attempt was made to detect, for example, any large-scale jet flapping caused by pulsed CJs. Details of the LDA configuration are contained in Table 1.

III. Results

To illustrate the level of detail achieved in the data set gathered during the present investigation, radial profiles in the near field ($x/D_n < 10$) of the primary jet are used. Only selected profiles are given here; the full data set is available in [36]. The clean jet data (i.e., unforced by any CJs) is provided first to establish the datum against which enhanced mixing performance should be judged. To investigate the effect of CJ penetration and interaction with the primary jet shear layer, measurements were carried out at two steady CJ supply total pressures of 2 and 3 bar. The total CJ mass flow rates at these operating conditions were 0.25 and 0.41% of the primary jet mass flow, representing a level that is considered to constitute an affordable engine bleed flow. The 2 bar pressure (implying choked CJ nozzles) leads to a velocity ratio (CJ/primary jet) of around one; this was found in [21] to guarantee close interaction between the bent over CJ trajectory (and its associated streamwise vorticity) and the primary jet shear layer. The corresponding momentum ($\rho_{cj}U_{cj}^2/\rho_j U_j^2$) and velocity ($U_{cj}/U_j$) ratios for the 2 and 3 bar runs were 1.35/1.4 and 2.27/1.39, respectively. Very little difference was observed in enhanced mixing performance between the two supply pressures (see [36] and next for details), so radial profile data given here are for 2 bar only. Pulsed CJs were therefore also operated at only the 2 bar condition but at three different Strouhal numbers of 0.1, 0.22, and 0.4 for a duty cycle of 0.64. Two azimuthal modes of pulsation were examined: axisymmetric (or in phase), referred to here as mode $m = 0$, and antisymmetric (180° out of phase), the $m = 1$ mode. Once again, only an illustrative sample of the data is provided.

Radial profiles are then compared between steady and pulsed CJs ($St = 0.22$, $\alpha = 0.64$, and mode $m = 0$ only) to quantitatively assess the near-field mixing changes that are brought about. Finally, to

Table 1 LDA measuring volume dimensions

	LDA 1 (green)	LDA 2 (blue)
Measurement volume diameter, mm	0.076	0.072
Measurement volume length, mm	1.192	1.131

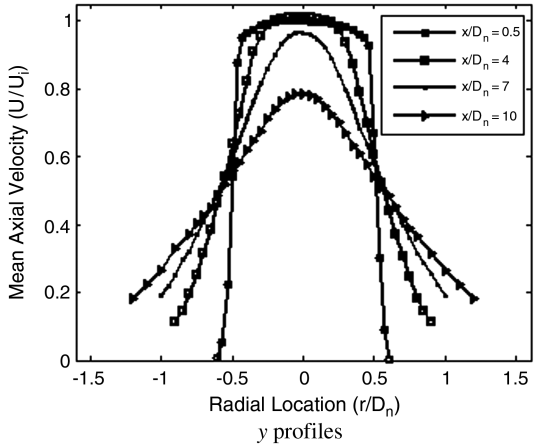

Fig. 9 Radial profiles of mean axial velocity at several axial locations (clean jet).

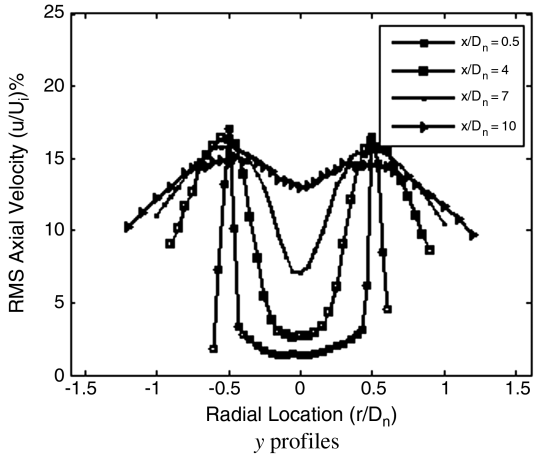

Fig. 10 Radial profiles of axial turbulence intensity at several axial locations (clean jet).

enable the most informative and direct comparison of the effect of the Strouhal number and azimuthal mode on mixing, axial traverse profiles taken along the primary jet centerline and lip line are examined; these best illustrate how jet velocity decay rate and entrainment are influenced. Note that, for clean jet flow, its axisymmetric nature means that measurements along y- or z-radial lines and y- or z-axial lip lines should be identical. For steady or pulsed CJ nozzles, both y and z directions have to be examined to capture a complete picture of flow development (note that, as indicated previously, the CJ nozzles are located and discharge in the z direction).

A. Radial Traverse Profiles

1. *Clean Jet*

Profiles for the mean axial velocity at several downstream stations for the clean jet case are shown in Fig. 9. Note that excellent symmetry was achieved in this data set; y and z profiles demonstrated close similarity so that only y profiles are shown in Fig. 9. Near the nozzle exit plane, the jet has a typical top-hat profile ($x/D_n = 0.5$) with a relatively thin annular shear layer. The shear layer spreads inward with axial distance, diminishing the radial width of the potential core. At $x/D_n = 4$, the centerline velocity is still at its nozzle exit level, but it has started to decrease at $x/D_n = 7$. Defining the potential core length as the point where U/U_j falls below 99% on the jet centerline leads to a potential core length of $6D_n$ typical of a high Re jet with a fully turbulent boundary layer at nozzle exit. The maximum mean velocity at $10D_n$ is $\sim$80% of U_j and, extrapolating the profile radially to zero velocity, implies entrainment has increased the jet diameter to $\sim 3.6D_n$ at this plane. The quantitative extent of improved near-field mixing when CJs are introduced is best judged by comparison against these clean jet data.

Figure 10 presents similar radial traverse data for the axial rms turbulence intensity, at the same downstream stations. Once again excellent symmetry was obtained, so only y profiles are presented. The peak values identify the regions of maximum production of turbulence due to the high strain rates in the shear layer. At the closest measurement station to the nozzle exit ($x/D_n = 0.05$, not shown here, see [36]), the peak value was already 14% (at $r/D_n = 0.5$); this increased to 16% by $x/D_n = 0.5$ and remained at this value throughout the near field. The radial movement of the outer/inner edges of the annular shear layer can be easily identified in these profiles. Mixing causes smoothing, so turbulence profiles become relatively flat by $x/D_n = 10$.

2. *Steady Control Jets*

Figure 11 shows that strong three-dimensional behavior results when steady CJs are switched on and interact with the primary jet shear layer. The changes from axisymmetric behavior in the z-direction profile are much greater than for the y direction. The effect is already apparent in the z profile at $x/D_n = 0.5$, which shows a noticeably compressed shape in comparison to the y-direction profile. By $x/D_n = 4$, the z profile already displays a Gaussian bell shape and a lower-than-nozzle-exit peak velocity, indicating the end of the potential core has already occurred. Using the definition given previously, the potential core length is $3.2D_n$, a reduction of $\sim$46% relative to the clean jet case. Note that a minor health warning should be given here: it is standard practice to determine the potential core length of jets from centerline conditions, and this practice is also

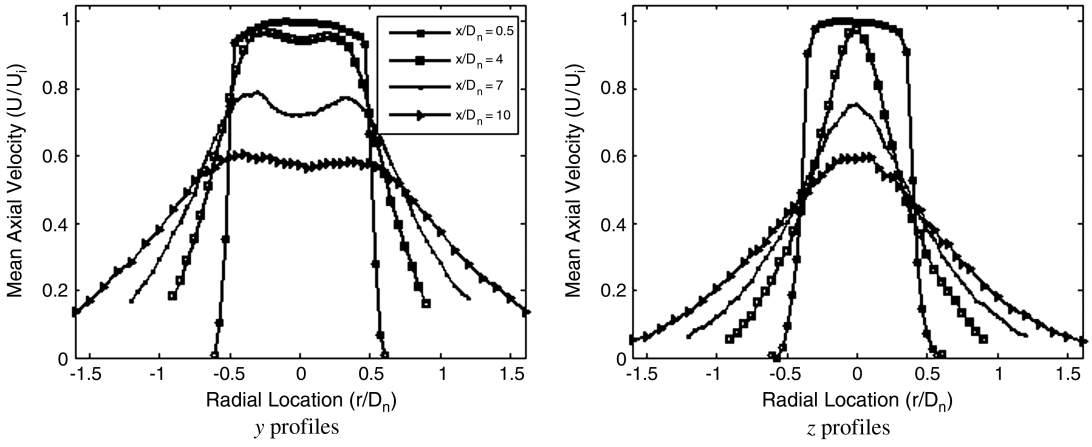

Fig. 11 Radial profiles of mean axial velocity at several axial locations (steady CJs).

followed here and leads to the 46% reduction quoted. However, when CJs (steady or pulsed) are introduced at momentum ratios for high effectiveness, this can lead to jet bifurcation. In this case, the centerline velocity no longer represents the maximum jet velocity, so to refer to this as the potential core end is slightly misleading. The axial location at which the maximum velocity anywhere in the jet falls below 99% of its nozzle exit value can only be determined by examining the full radial profile data. This effect is visible in the y profiles shown in Fig. 11. In contrast to the z profile, the shear layer has expanded in the y direction. At $x/D_n = 4$, the y profile shows an offcenterline double-peaked shape. This indicates a mild bifurcation of the jet core has taken place. The double-peaked shape grows in amplitude for a short distance, but by $x/D_n = 10$, the profile is rather flat. The peak axial velocity at $x/D_n = 10$ is $\sim 0.61 U_j$, a reduction of some 25% compared with the clean jet value. The two orthogonal traverse profiles indicate that the jet cross section is elliptic, with major and minor axis dimensions at $x/D_n = 10$ of $4.7D_n$ and $4.2D_n$. Both of these are greater than the clean jet figure ($3.6D_n$): the peripheral length of the jet/ambient interface has increased with the introduction of steady CJs by $\sim$25% over the clean jet case. These figures provide clear evidence of and explain the cause of the enhanced mixing and jet spread.

Figure 12 presents data for the axial turbulence intensity with steady CJs for direct comparison with Fig. 10. The departures from axial symmetry are even more visible in the turbulence data. Already, at $x/D_n = 0.5$, the inward/outward movement along the z and y directions is evident, and this strengthens with downstream distance, with the inward movement more exaggerated. The peak turbulence intensity level is hardly changed, although its location has now moved away from the lip line region; the turbulence levels in the z direction in the outer region are, in general, $\sim$20% increased compared with the clean case, which will aid increased entrainment.

3. *Pulsed Control Jets*

Radial profile data for mean velocity and axial rms are shown in Figs. 13 and 14 for pulsed CJs operating at $St = 0.22$, $\alpha = 0.64$, and $m = 0$. The z-direction contraction/y-direction expansion observed with steady CJs is also seen with pulsed CJs, with contraction being somewhat milder in the pulsed case (which is an improved result, as jet cross-sectional contraction is undesirable). The evidence of a double-peaked profile in the y direction is also, as a consequence, much weaker. Interpolating the potential core length (seen better in centerline turbulence data; see next) indicates a length of $3D_n$, a 50% reduction compared with the clean jet, a slightly greater reduction than the steady jet case. The peak velocity at $x/D_n = 10$ is $0.61U_j$; i.e., a 25% reduction compared with the clean jet value, the same as for steady CJs. Evidence of an elliptical jet cross section is again visible at the furthest downstream station, with major/minor axes being $4.8D_n$ and $4.5D_n$ (the latter confirming the weaker contraction effect); the jet peripheral interface with ambient has thus increased by 30%, a slight improvement on the steady CJ value. The rms plots show similar features to Fig. 12 for steady CJs; noticeable differences are 1) the peak rms value occurs in the z direction in both steady and pulsed cases but reaches 24% for pulsed jets, compared with 18% for steady CJs; and 2) at further downstream stations, $x/D_n = 4$, 7, and 10, the pulsed rms levels are generally higher than for steady CJs over the whole profile. The cumulative effect of pulsing the CJs (at essentially the same steady mass flow rate as in the steady CJ case) is thus much weaker evidence of bifurcation, an increased jet/ambient periphery, and higher turbulence levels.

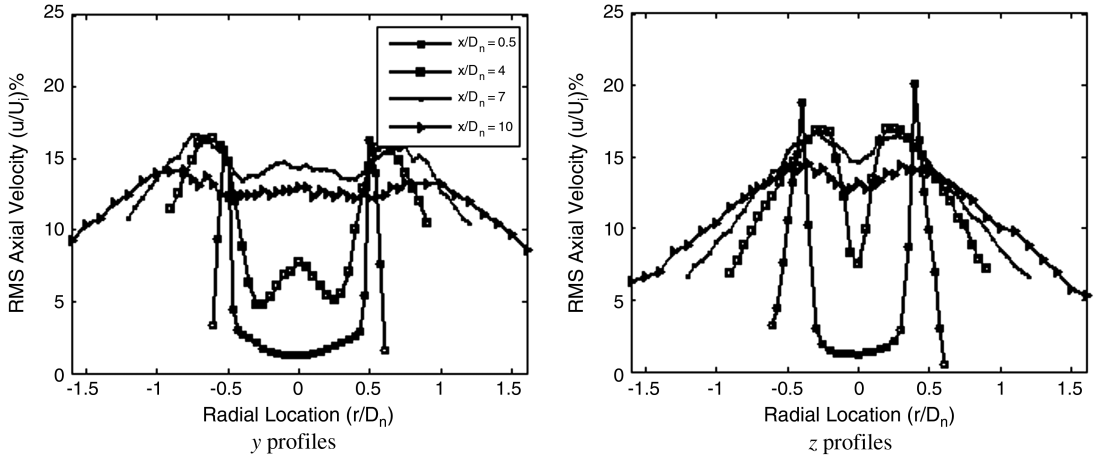

Fig. 12 Radial profiles of axial turbulence intensity at several axial locations (steady CJs).

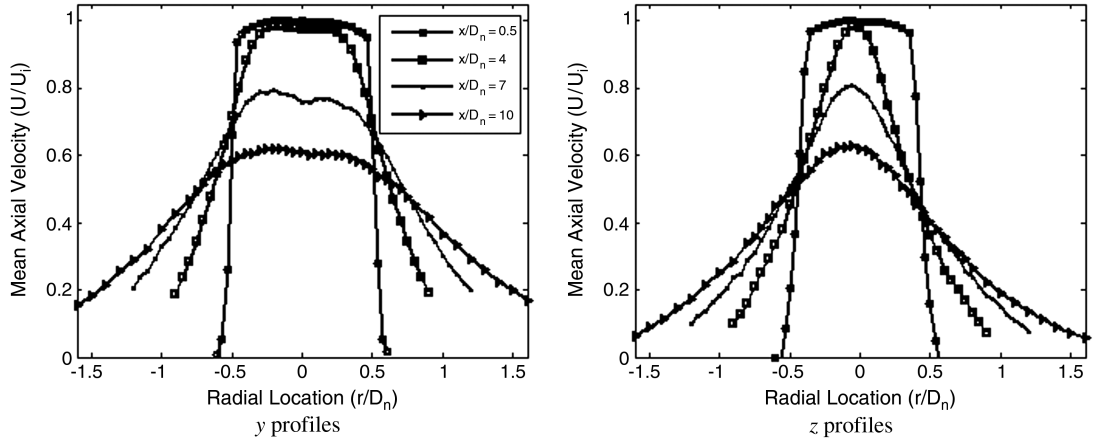

Fig. 13 Radial profiles of mean axial velocity at several axial locations (pulsed CJs).

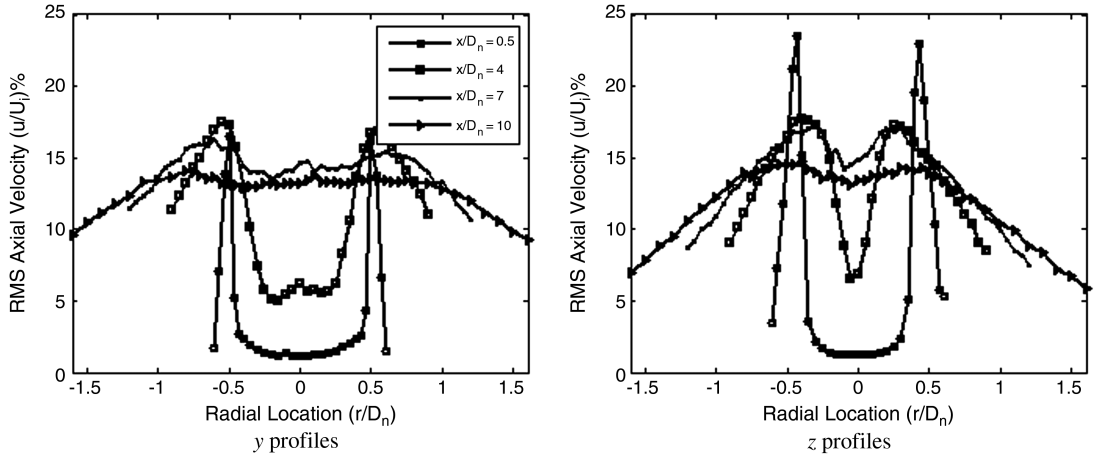

Fig. 14 Radial profiles of axial turbulence intensity at several axial locations (pulsed CJs).

B. Axial Traverse Profiles: Centerline and Nozzle Lip Line

1. Steady Control Jets: Effect of Control Jet Pressure

Centerline and lip line traverse measurements for steady CJs at two supply pressures are shown in Fig. 15. The lip line is the radial line emanating from the nozzle exit wall location: i.e., $r/D_n = 0.5$. Measurements along the lip line are valuable, in that this is the zone of high turbulence generation, and hence high ambient mass entrainment, into the primary jet in the initial free shear-layer

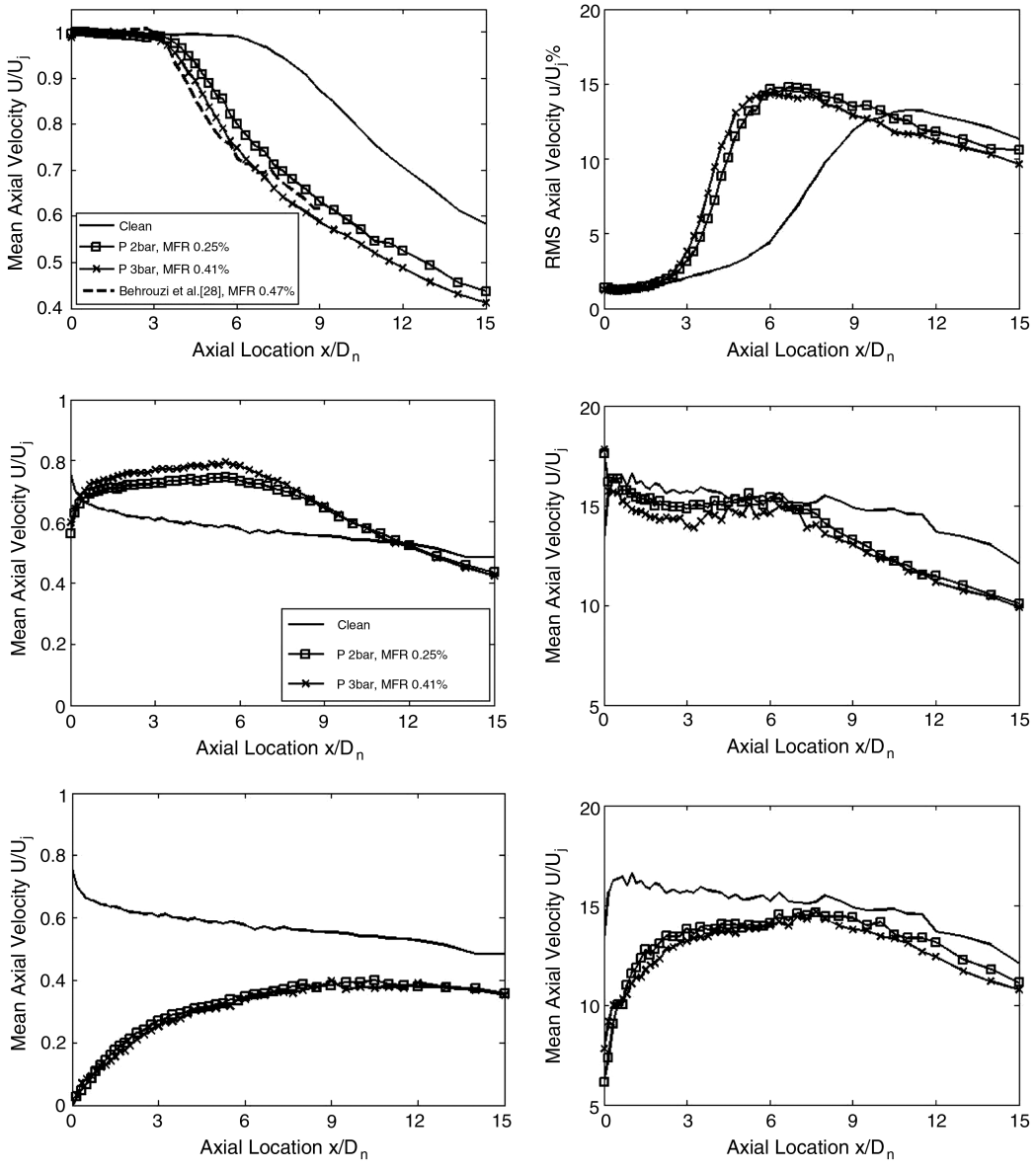

Fig. 15 Centerline (top), *y* lip line (middle), and *z* lip line (bottom) characteristics (clean and steady CJs). MFR = mass flow ratio = $\dot{m}_{\mathrm{CJs}}/\dot{m}_{\mathrm{PJ}}$.

region. For comparative purposes, the clean jet data are also included, as are the mean velocity centerline data taken by Behrouzi and McGuirk [27] in the same experimental facility but with an alternative CJ system, to demonstrate the good repeatability achieved. The clean jet potential core length of $6D_n$ has decreased on introduction of steady CJs to $3.2D_n$ and $3D_n$ for operating pressures of 2 and 3 bar, respectively: reductions of 46 and 50%. In the fully merged jet region, the centerline velocity at $x/D_n = 10$ has reduced from $0.81U_j$ to $0.59U_j$ and $0.56U_j$. After 10 nozzle diameters, the decay rate for all cases becomes asymptotic, showing that CJs only influence the near field of the primary jet. The turbulent axial rms velocity data illustrate that centerline turbulence levels are modified by steady CJs. For the clean jet, the rms velocity at nozzle exit is 1% of U_j, but this increases steadily to 6% at $x/D_n = 6$; the axial gradient then steepens significantly, since the annular shear layer has now reached the centerline, marking the end of the potential core. The increase in turbulence up to this point is caused by irrotational velocity unsteadiness induced by the fluctuating inner edge of the shear layer rather than representing genuine shear-generated turbulence. With CJ forcing, the rms intensity on the centerline increases much earlier and reaches its saturation point much quicker than in the clean jet. The peak rms velocities for clean, 2 bar, and 3 bar CJs are 12, 14, and 16% of U_j. All three curves show downstream merging and asymptotic behavior, illustrating once again that CJs only influence the first ~10 diameters downstream of the nozzle exit. Along both y and z lip lines, the clean jet mean velocity data show a steady decrease, indicating the gradual spread of the jet outer edge as it mixes with the ambient. In contrast, the data from the flows with steady CJs show an increase. For the y lip line, the increase peaks at $\sim 6D_n$, whereas the z lip line shows a more gradual rise, followed after $10D_n$ by a slow decrease (note the zero velocity at the origin in the z direction is due to this being the entry point of the radially oriented CJs). The explanation for increased axial velocity on the y lip line is the rapid outward movement of the core primary jet fluid in the y direction caused by the CJ-induced inward contraction in the z direction, as described previously. Similarly, the axial velocity magnitude along the z lip line, remaining always smaller than for the clean jet, is consistent with primary jet contraction in the plane of CJ entry. The rms turbulence measurements on the lip lines show only little difference to clean jet data for the first $6D_n$, which is again consistent with increased mean velocity on the y lip line being caused by a displacement rather than an enhanced entrainment effect. In fact, in general, the turbulence levels with CJs are either similar or smaller than the clean jet data, which implies that increased primary jet entrainment is due much more to an increased interface for ambient fluid to be entrained than increased turbulence activity. In terms of effectiveness (i.e., changed primary jet behavior as a consequence of the increased CJ mass flow rate), the 3 bar CJ results do not seem to

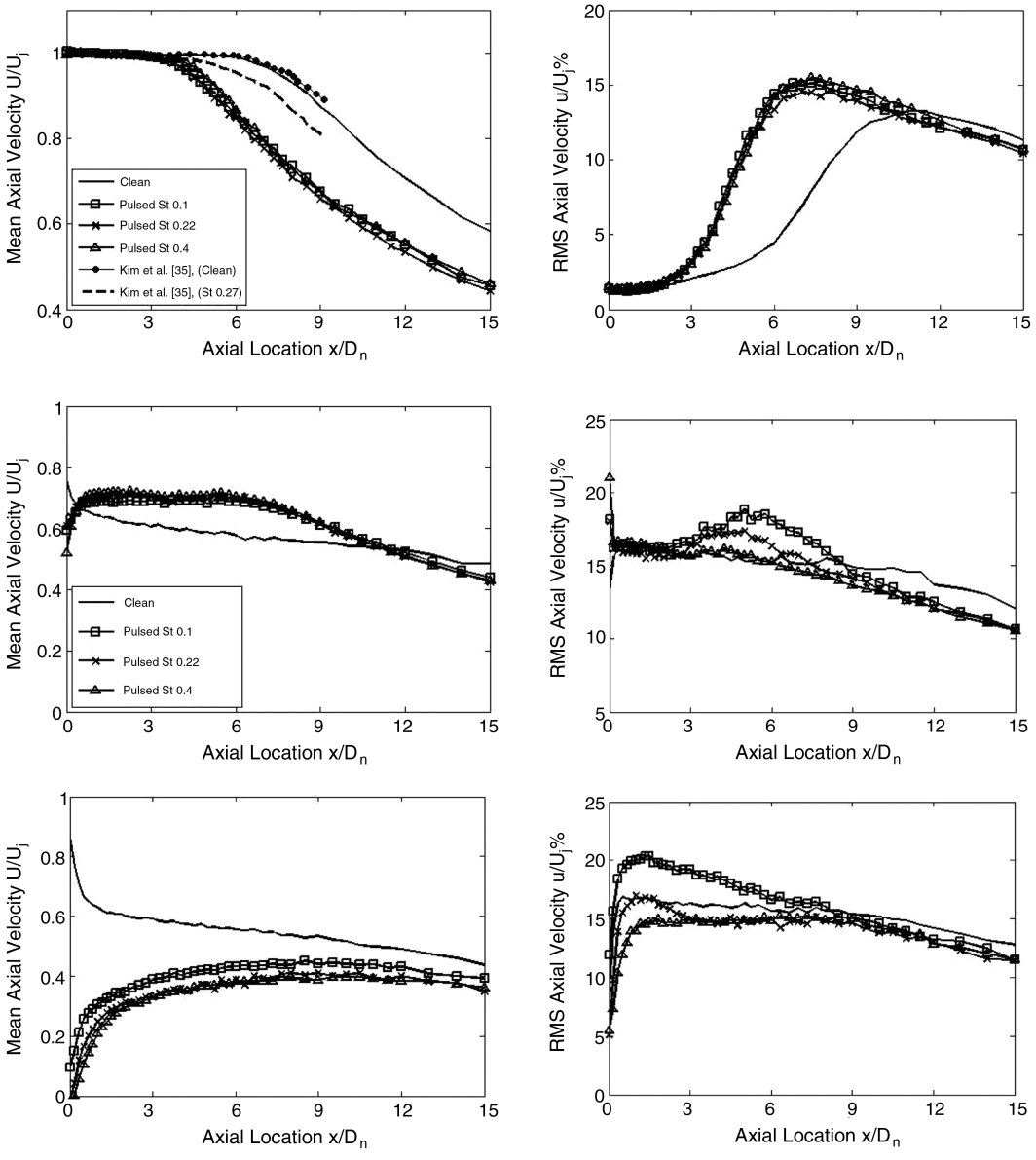

Fig. 16 Effect of pulsed CJ Strouhal number: centerline (top), y lip line (middle), and z lip line (bottom).

justify the extra engine bleed, since the performance is hardly different to the 2 bar CJ case.

2. *Pulsed Control Jets: Effect of Strouhal Number*

The normalized profiles along centerline and the y and z lip lines are shown in Fig. 16 for pulsed CJs at all Strouhal numbers tested. It can be seen that the influence of St was rather small over the 0.1–0.4 range. There is some evidence (e.g., centerline behavior) that the $St = 0.22$ case is slightly better than the other two St values, but the differences are marginal. This is also true of the rms turbulence behavior. Lip line variations with St are greater, showing, for example, that the $St = 0.1$ pulsation produces the highest turbulence levels in the region $x/D_n < 6$. One explanation for this could be that lower pulsation frequency allows the unsteady flow created by each pulse of injected CJ fluid during the on part of the cycle to persist for a longer time before mixing with neighboring pulses than at higher frequencies. This would also explain why the $St = 0.44$ data are the closest to the steady CJ data. It should be remembered that these tests were done at constant duty cycle. Further tests at lower values of α would be useful to explore this pulse separation effect further. A comparison is also provided in the mean centerline plot in Fig. 16, with the pulsed excitation data of Kim et al. [35]. The measurements reported in [35] were for a $M = 0.9$ primary jet but used eight LAFPAs rather than two pulsed CJs, as in the present work. The clean jet data compare very well with the current measurements, showing that the baseline jet in [35] and in the present work are identical. However, it can be seen that the present case of two CJs is more effective at inducing rapid mixing and enhanced centerline velocity decay. This may be due to the target application in [35] being for noise control rather than mixing enhancement, implying multiple excitation sites rather than the two selected here. As mentioned earlier, a smaller number of perturbation sites gives more opportunity for macroscale jet cross-sectional modification, which is argued as the primary mechanism for increased entrainment over the clean jet case in the current context.

3. *Pulsed Control Jets: Effect of Mode Number*

Pulsation mode effects are compared in Fig. 17. For the present measurements, axisymmetric ($m = 0$) and antisymmetric ($m = 1$) mode data are shown for $St = 0.22$ and $\alpha = 0.64$. Note the antisymmetric mode ($m = 1$) was activated by operating the CJs with a phase difference of 180°; however, since the duty cycle α was greater than 0.5, this meant that there was an overlapping period where both CJs were on at the same time. The figure also includes results from Kim et al. [35] for $m = 0$, 1, and ± 1, at the Strouhal number where maximum reduction in potential core length was observed. The $m = 0$ case allows a direct comparison with the current results; the reason both $m = 1$ and $m = \pm 1$ from [35] are

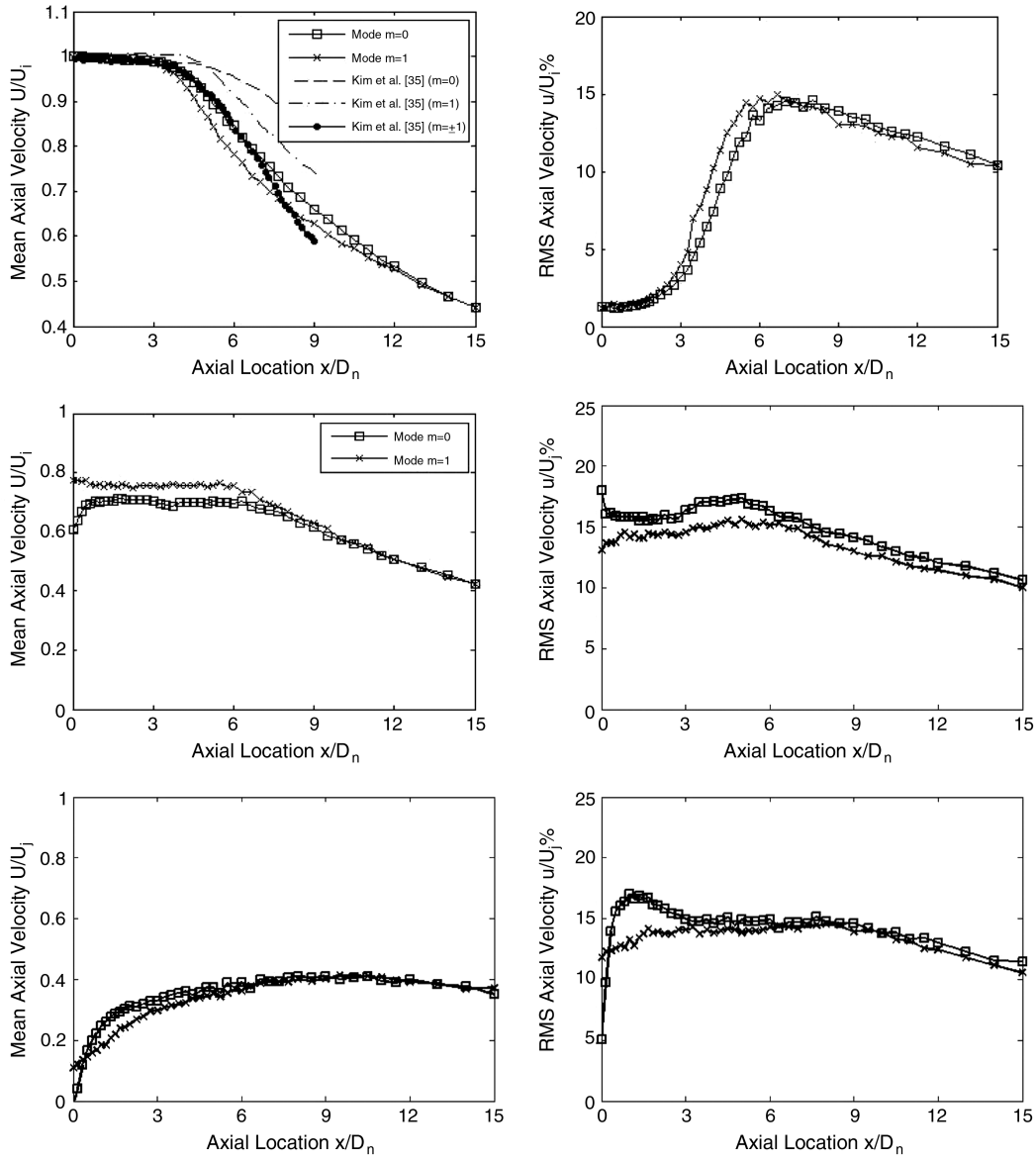

Fig. 17 Effect of pulsed CJ mode number: centerline (top), y lip line (middle), and z lip line (bottom).

presented here is to emphasize that comparisons from tests conducted in different facilities need to be made with care. The azimuthal mode $m = 1$ in [35] was achieved by operating successive actuators with a phase delay of 45°; the $m = \pm 1$ operation mode used in [35] was the closest to the current $m = 1$ operation mode. In general, the present results show a small gain in performance (increased decay and shorter potential core length; see centerline data) for mode $m = 1$. The improved performance of the antisymmetric mode ($m = 1$) in the current data over the mixed mode $m = \pm 1$ results of [35] again emphasizes that the number of excitation sites used in the current investigation is more effective in enhancing the mixing of the primary jet with the ambient, giving more opportunity for macroscale jet cross-sectional modification. Slightly higher velocity along the y lip line and higher turbulence levels also illustrate the improved performance of the current antisymmetric forcing. However, this gain, based on centerline and lip line data, should be taken with caution, since this might have been caused by flapping of the jet core. More investigation of the physical changes in the primary jet due to antisymmetric forcing is therefore needed.

C. Jet Spread

A normalized jet edge radius, defined here for convenience as the radial distance from the primary jet axis to the location where the mean axial velocity is 0.4 of its centerline value, is plotted in Fig. 18. This may be used to compare the effectiveness of various CJ operating conditions. The primary jet contraction/expansion described previously is easily identified in Fig. 18. The effectiveness of steady and pulsed CJs as alternative mixing enhancement devices may be directly compared here. The spread observed in the 3 bar steady CJ case was essentially identical to the 2 bar, so only the latter is shown. Similarly, the $St = 0.22$ pulsed CJs were found to be the most effective in terms of overall spreading of the jet (i.e., to produce maximum y direction spreading with reduced z-direction contraction) compared with $St = 0.1$ or 0.4; hence, only data for $St = 0.22$ are presented. Expansion and contraction of the jet radius in the y and z directions caused by the CJs are clearly evident. The contraction of the primary jet along the z direction with the pulsed CJs is clearly less severe compared with the steady CJs. The expansion caused by both steady and pulsed CJ devices in the y direction is identical up to $x/D_n = 5$, beyond which the pulsed CJs are more effective in enhancing the jet spread. This enhanced y-direction spread and lower z-direction contraction caused by pulsed CJs compared with steady CJs shows that pulsed CJs are more efficient at enhancing the spread of the jet and increasing the mixing of the jet with the ambient. The far-field spreading rate of a clean jet is given in Pope [37] as 0.096. Note that the present clean jet data in Fig. 18 have not yet achieved this rate of spread, with the jet edge growing at only around 50% of this value; this confirms the near-field nature of the clean jet behavior: the far-field spreading rate would only be reached at $x/D_n > 20$. The CJ excited cases show that the far-field spreading rate is achieved by $x/D_n = 3$, demonstrating that CJ excitation significantly shortens the distance to achieve the far-field spreading rate.

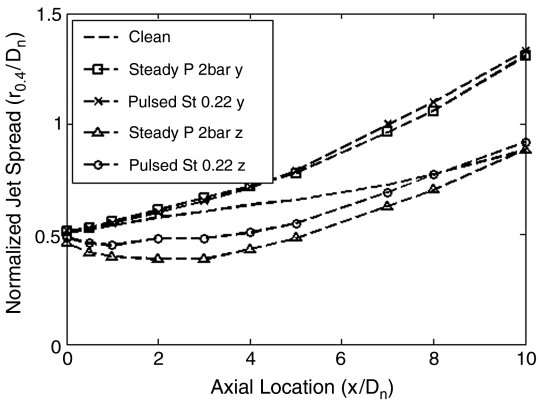

Fig. 18 Jet spreading: clean, steady, and $St = 0.22$ pulsed CJs.

IV. Conclusions

The focus of the work presented here has been to investigate the effectiveness of CJs for enhanced mixing on high Re, high M jets. This study has shown that use of CJs (steady and pulsed) is an effective mixing enhancement technique. For example, the results have shown that significant potential core length reduction can be achieved by using CJs. When CJs are introduced, the jet cross section becomes highly asymmetric; the jet spreading rate contracts in the plane of CJ entry but increases considerably in the orthogonal plane. One significant observation is that this elliptic cross section induced by the CJs is an important factor in increased near-field mixing, as well as the enhanced turbulence levels created. Pulsed CJs can improve performance: potential core length reduction of 40% (steady) or 50% (pulsed), jet cross-section increase of 25% (steady) or 30% (pulsed), and peak turbulence levels of 18% (steady) or 24% (pulsed). The Strouhal number for optimum mixing was not found to be very sensitive in the range studied, but for the present case, $St = 0.22$ marginally gave the best results. Similarly, there was some benefit from antisymmetric (mode $m = 1$) pulsation. Comparison with the previous data of Kim et al. [35], who used plasma actuators, showed improved mixing performance using CJs, although the larger number of actuators used in [35], driven by their interest in jet noise reduction rather than mixing, certainly contributed to this result. The data presented here, particularly because of the turbulence information provided, are considered valuable validation data for CFD studies of jet mixing. More work is needed in several areas; in particular, the effect of duty cycle was not studied in the present work, and it would be useful to build on the preferred CJ parameters identified here (CJ pressure, St, and mode number) to investigate the effect of duty cycle on mixing performance.

References

[1] Knowles, K., and Saddington, A. J., "A Review Of Jet Mixing Enhancement For Aircraft Propulsion Applications," *Proceedings of the Institution of Mechanical Engineers, Part G: Journal of Aerospace Engineering*, Vol. 220, No. 2, 2006, pp. 103–127. doi:10.1243/09544100G01605

[2] Tillman, T. G., Patrick, W. P., and Paterson, R. W., "Enhanced Mixing Of Supersonic Jets," *Journal of Propulsion and Power*, Vol. 7, No. 6, 1991, pp. 1006–1014. doi:10.2514/3.23420

[3] Samimy, M., Kim, J. H., and Clancy, P. S., "Passive Control Of Supersonic Rectangular Jets Via Nozzle Trailing-Edge Modifications," *AIAA Journal*, Vol. 36, No. 7, 1998, pp. 1230–1239. doi:10.2514/2.504

[4] Bradbury, L. J. S., and Khadem, A. H., "Distortion Of A Jet By Tabs," *Journal of Fluid Mechanics*, Vol. 70, No. 4, 1975, pp. 801–813. doi:10.1017/S0022112075002352

[5] Samimy, M., Zaman, K. B. M. Q., and Reeder, M. F., "Effect Of Tabs On The Flow And Noise Field Of An Axisymmetric Jet," *AIAA Journal*, Vol. 31, No. 4, 1993, pp. 609–619. doi:10.2514/3.11594

[6] Carletti, M. J., Rogers, C. B., and Parekh, D. E., "Parametric Study Of Jet Mixing Enhancement By Vortex Generators, Tabs And Deflector Plates," *Proceedings of 1996 ASME Fluids Engineering Division Summer Meeting, Part 2*, San Diego, CA, American Soc. of Mechanical Engineers, Fairfield, NJ, 1996, pp. 303–333.

[7] Hu, H., Saga, T., and Koboyashi, T., "Passive Control Of Jet Mixing Flows By Using Vortex Generators," *Proceedings of the 6th International Symposium on Fluid Control, Measurement and Visualization*, Sherbrooke, Canada, 2000.

[8] Crow, S. C., and Champagne, F. H., "Orderly Structure In Jet Turbulence," *Journal of Fluid Mechanics*, Vol. 48, No. 3, 1971, pp. 547–591. doi:10.1017/S0022112071001745

[9] Raman, G., and Cornelius, D., "Jet Mixing Control Using Excitation From Miniature Oscillating Jets," *AIAA Journal*, Vol. 33, No. 2, 1995, pp. 365–368. doi:10.2514/3.12444

[10] Wiltse, J. M., and Glezer, A., "Manipulation Of Free Shear Layers

Using Piezoelectric Actuators," *Journal of Fluid Mechanics*, Vol. 249, 1993, pp. 261–285.
doi:10.1017/S002211209300117X

[11] Zaman, K. B. M. Q., Reeder, M. F., and Samimy, M., "Control Of An Axisymmetric Jet Using Vortex Generators," *Physics of Fluids*, Vol. 6, No. 2, 1994, pp. 778–793.
doi:10.1063/1.868316

[12] Behrouzi, P., and McGuirk, J., "Experimental Studies Of Tab Geometry Effects On Mixing Enhancement Of An Axisymmetric Jet," *JSME International Journal. Series B, Fluids and Thermal Engineering.*, Vol. 41, No. 4, 1998, pp. 908–917.

[13] Foss, J. K., and Zaman, K. B. M. Q., "Large And Small-Scale Vortical Motions In A Shear Layer Perturbed By Tabs," *Journal of Fluid Mechanics*, Vol. 382, 1999, pp. 307–329.
doi:10.1017/S0022112098003887

[14] Bohl, D. G., and Foss, J. F., "Near Exit Plane Effects Caused By Primary And Primary Plus Secondary Tabs," *AIAA Journal*, Vol. 37, No. 2, 1999, pp. 192–201.
doi:10.2514/2.713

[15] Hu, H., Saga, T., Kobayashi, T., and Taniguchi, N., "Stereoscopic PIV Measurement Of A Jet Flow With Vortex Generating Tabs," *10th International Symposium on Flow Visualization*, Kyoto, Japan, 2002.

[16] Johnston, J. P., and Nishi, M., "Vortex Generator Jets: Means For Flow Separation Control," *AIAA Journal*, Vol. 28, No. 6, 1990, pp. 989–994.
doi:10.2514/3.25155

[17] Bray, T. P., and Garry, K. P., "Optimization Of Air Jet Vortex Generators With Respect To System Design Parameters," *The Aeronautical Journal*, Vol. 103, 1999, pp. 475–480.

[18] Davis, M. R., "Variable Control Of Jet Decay," *AIAA Journal*, Vol. 20, No. 5, 1982, pp. 606–609.
doi:10.2514/3.7934

[19] Lardeau, S., Collin, E., Lamballais, E., Delville, J., Barre, S., and Bonnet, J. P., "Analysis Of A Jet-Mixing Layer Interaction," *International Journal of Heat and Fluid Flow*, Vol. 24, No. 4, 2003, pp. 520–528.
doi:10.1016/S0142-727X(03)00046-8

[20] Collin, E., Barre, S., and Bonnet, J. P., "Experimental Study Of A Supersonic Jet-Mixing Layer Interaction," *Physics of Fluids*, Vol. 16, No. 3, 2004, pp. 765–778.
doi:10.1063/1.1644574

[21] Behrouzi, P., and McGuirk, J., "Jet Mixing Enhancement Using Fluid Tabs," 2nd AIAA Flow Control Conference, Portland, OR, AIAA Paper 2004-2401, 2004.

[22] Chauvet, N., Deck, S., and Jacquin, L., "Numerical Study Of Mixing Enhancement In A Supersonic Round Jet," *AIAA Journal*, Vol. 45, No. 7, 2007, pp. 1675–1687.
doi:10.2514/1.27497

[23] Crow, S. C., and Champagne, F. H., "Orderly Structure in Jet Turbulence," *Journal of Fluid Mechanics*, Vol. 48, No. 3, 1971, pp. 547–591.
doi:10.1017/S0022112071001745

[24] Parekh, D. E., Kibens, V., Glezer, A., Wiltse, J. M., and Smith, D. M., "Innovative Jet Flow Control: Mixing Enhancement Experiments," AIAA Paper 1996-0308, 1996.

[25] McKinney, G., "*Research Highlights*," U.S. Air Force Office of Scientific Research Communications and Technical Information, Arlington, VA, Sept.–Oct. 1998.

[26] Ibrahim, M. K., Kunimura, R., and Nakamura, Y., "Mixing Enhancement Of Compressible Jets By Using Unsteady Microjets As Actuators," *AIAA Journal*, Vol. 40, No. 4, 2002, pp. 681–688.
doi:10.2514/2.1700

[27] Behrouzi, P., and McGuirk, J., "Flow Control Of Jet Mixing Using A Pulsed Fluid Tab Nozzle," 3rd AIAA Flow Control Conference, San Francisco, CA, AIAA Paper 2006-3509, 2006.

[28] Behrouzi, P., Feng, T., and McGuirk, J. J., "Active Control Of Jet Mixing Using Steady And Pulsed Fluid Tabs," *Proceedings of the Institution of Mechanical Engineers. Part I, Journal of Systems and Control Engineering*, Vol. 222, No. 5, 2008, pp. 381–392.
doi:10.1243/09596518JSCE543

[29] Johari, H., Paecheo-Tougas, M., and Hermanson, J. C., "Penetration And Mixing Of Fully Modulated Turbulent Jets In Crossflow," *AIAA Journal*, Vol. 37, No. 7, 1999, pp. 842–850.
doi:10.2514/2.7532

[30] Johari, H., "Scaling Of Fully Pulsed Jets In Crossflow," *AIAA Journal*, Vol. 44, No. 11, 2006, pp. 2719–2725.
doi:10.2514/1.18929

[31] Suzuki, H., Kasagi, N., and Suzuki, Y., "Active Control Of An Axisymmetric Jet With Distributed Electromagnetic Flap Actuators," *Experiments in Fluids*, Vol. 36, No. 3, 2004, pp. 498–509.
doi:10.1007/s00348-003-0756-0

[32] Samimy, M., Adamovich, I., Webb, B., Kastner, J., Hileman, J., Keshav, S., and Palm, P., "Development And Characterisation Of Plasma Actuators For High Speed Jet Control," *Experiments in Fluids*, Vol. 37, No. 4, 2004, pp. 577–588.
doi:10.1007/s00348-004-0854-7

[33] Samimy, M., Kim, J.-H., Kastner, J., Adamovich, I., and Utkin, Y., "Active Control Of A Mach 0.9 Jet For Noise Mitigation Using Plasma Actuators," *AIAA Journal*, Vol. 45, No. 4, 2007, pp. 890–901.
doi:10.2514/1.27499

[34] Samimy, M., Kim, J.-H., Kastner, J., Adamovich, I., and Utkin, Y., "Use Of Localised Arc Filter Plasma Actuators For High Speed Jet Control," *Journal of Fluid Mechanics*, Vol. 578, May 2007, pp. 305–330.
doi:10.1017/S0022112007004867

[35] Kim, J.-H., Kastner, J., and Samimy, M., "Active Control Of A High Reynolds Number Mach 0.9 Axisymmetric Jet," *AIAA Journal*, Vol. 47, No. 1, 2009, pp. 116–127.
doi:10.2514/1.36801

[36] Kamran, M. A., "Manipulation of High Mach Number Shear Layers Using Control Jets," Ph.D. Thesis, Loughborough Univ., U.K., 2009.

[37] Pope, S. B., *Turbulent Flows*, Cambridge Univ. Press, New York, 2000.

S. Fu
Associate Editor